

This discussion paper is/has been under review for the journal Atmospheric Chemistry and Physics (ACP). Please refer to the corresponding final paper in ACP if available.

# Simultaneous occurrence of polar stratospheric clouds and upper-tropospheric clouds caused by blocking anticyclones

M. Kohma<sup>1</sup> and K. Sato<sup>1</sup>

<sup>1</sup>Department of Earth and Planetary Science, The University of Tokyo, Tokyo, Japan

Received: 12 June 2012 – Accepted: 1 August 2012 – Published: 10 August 2012

Correspondence to: M. Kohma (kohmasa@eps.s.u-tokyo.ac.jp)

Published by Copernicus Publications on behalf of the European Geosciences Union.

## Polar stratospheric clouds and upper-tropospheric clouds

M. Kohma and K. Sato

Title Page

Abstract

Introduction

Conclusions

References

Tables

Figures



Back

Close

Full Screen / Esc

Printer-friendly Version

Interactive Discussion

## Abstract

This study statistically examines the simultaneous appearance of polar stratospheric clouds (PSCs) and upper tropospheric clouds (UCs) using satellite lidar observations for five austral winters of 2007–2011. The time series of PSC occurrence in the height range of 15–25 km are significantly correlated with those of UC in 9–11 km. The UCs observed simultaneously with PSCs reported in previous case studies are possibly located around and slightly above the tropopause ( $\sim 7$ – $8$  km) rather than in the troposphere. It is shown that the simultaneous occurrence of PSCs and UCs is frequently associated with blocking highs having large horizontal scales (several thousand kilometers) and tall structure (up to a height of  $\sim 15$  km). The longitudinal variation of blocking high frequency accords well with that of the simultaneous occurrence frequency of PSCs and UCs. This coincidence is clearer when the analysis is limited to the latitudinal regions inside the stratospheric polar vortex. This fact suggests that the blocking highs provide a preferable condition for the simultaneous occurrence of PSCs and UCs. Moreover, PSC compositions are investigated as a function of relative-longitude of the anticyclones including blocking highs. It is seen that relatively high proportions of STS (super-cooled ternary solutions), Ice, and Mix2 (mixture of nitric acid trihydrate and STS) types are distributed to windward of, around, and to leeward of the anticyclones in the westerly background flows, respectively.

## 1 Introduction

Polar stratospheric clouds (PSCs), which appear in the polar stratospheric winter, have significant roles in polar stratospheric ozone depletion. They provide an environment for the heterogeneous reactions that convert stable chlorine and bromine reservoirs to active forms, and lead irreversible removal of  $\text{NO}_y$  from the lower stratosphere (denitrification) (Solomon, 1999). From lidar observations, it is shown that PSCs are mainly composed of nitric acid trihydrate (Type 1a, NAT), super-cooled ternary solution (Type 1b,

## Polar stratospheric clouds and upper-tropospheric clouds

M. Kohma and K. Sato

Title Page

Abstract

Introduction

Conclusions

References

Tables

Figures

⏪

⏩

◀

▶

Back

Close

Full Screen / Esc

Printer-friendly Version

Interactive Discussion



STS), and/or ice particles (Type 2) (Lowe and MacKenzie, 2008). Large NAT particles are considered to be responsible for efficient denitrification due to their rapid gravitational sedimentation (Jensen et al., 2002; Fueglistaler et al., 2002; Lambert et al., 2012).

5 PSCs are strongly modulated by atmospheric waves such as planetary waves, synoptic-scale waves and gravity waves (Teitelbaum et al., 2001; Carslaw et al., 1999; Eckermann et al., 2009; McDonald et al., 2009; Alexander et al., 2011; Kohma and Sato, 2011). Teitelbaum et al. (2001) showed that PSCs and synoptic-scale ozone minima appear simultaneously with synoptic-scale anticyclones around the tropopause in  
10 the Northern Hemisphere. They concluded that anticyclones near the tropopause have a primary role in the Arctic PSC occurrence. Using long-term satellite observations including Stratospheric Aerosol Measurement II, Stratospheric Aerosol and Gas Measurement II, and Polar Ozone and Aerosol Measurement II/III, Fromm et al. (2003) also confirmed that Arctic PSCs are frequently associated with the elevated tropopause  
15 (~10 km), which is attributable to anticyclones near the tropopause (Wirth, 2000). Anticyclonic potential vorticity (PV) anomalies near the tropopause are associated with low temperatures above (e.g. Holton, 2004): a PV anomaly at one level yields nonzero geopotential anomalies at levels above and below. The amplitude of geopotential anomaly takes its maximum at the level of the PV anomaly. As temperature anomaly  
20 is proportional to the vertical derivative of geopotential anomaly, an anticyclonic PV anomaly at one level is accompanied with low (high) temperatures above (below) it.

Using Challenging Mini-Satellite Payload (CHAMP) radio occultation observations, McDonald et al. (2009) showed that gravity waves increase the frequency of temperatures below the NAT equilibrium temperature in June in the Antarctic, in particular  
25 around the Antarctic Peninsula, which is a mountain wave “hotspot”. Kohma and Sato (2011) quantified the contribution of each type of waves to the PSC areal extent in both hemispheres using a temperature threshold based on temperatures from reanalysis data and GPS radio occultation observations and mixing ratios of HNO<sub>3</sub> and H<sub>2</sub>O from microwave limb sounder observations. They showed that planetary-scale temperature

**Polar stratospheric clouds and upper-tropospheric clouds**

M. Kohma and K. Sato

Title Page

Abstract

Introduction

Conclusions

References

Tables

Figures



Back

Close

Full Screen / Esc

Printer-friendly Version

Interactive Discussion



## Polar stratospheric clouds and upper-tropospheric clouds

M. Kohma and K. Sato

Title Page

Abstract

Introduction

Conclusions

References

Tables

Figures

⏪

⏩

◀

▶

Back

Close

Full Screen / Esc

Printer-friendly Version

Interactive Discussion

perturbations have a great contribution to PSC areal extent in the latitude range of 55° S–70° S while the contribution of synoptic-scale perturbation is large only around an altitude of 12 km. Compositions of PSCs are also affected by atmospheric waves, in particular by gravity waves (e.g. Carslaw et al., 1998; Höphner et al., 2006; Eckermann et al., 2009). Höphner et al. (2006) examined a sudden occurrence of circumpolar NAT distribution in June 2003 and attributed it to the heterogeneous nucleation on ice particles formed in a low temperature perturbation associated with mountain waves over the Antarctic Peninsula. From COSMIC/FORMOSAT observations in the Southern Hemisphere, Alexander et al. (2011) showed that ice and NAT PSCs are more frequent when and where the variances of temperature fluctuations associated with gravity waves are large.

Recent studies using satellite observations (Palm et al., 2005; Wang et al., 2008; Adhikari et al., 2010) reported that PSCs in the Antarctic are frequently observed simultaneously with upper tropospheric clouds (UCs). Palm et al. (2005) suggested a possible contribution of tropospheric disturbances to the formation of PSCs. Adhikari et al. (2010) examined PSC compositions and showed that the fraction of ice PSCs increases in association with the high and deep tropospheric cloud. However, the mechanisms causing the simultaneous occurrence of PSCs and UCs are still unclear. In addition, because the UCs that are simultaneously observed with PSCs tends to be mainly located near the tropopause (~7–8 km in the polar winter), it should be ascertained whether the UCs are actually “tropospheric” clouds.

This study statistically examines the frequency of simultaneous observations of PSCs and UCs using satellite lidar (the Cloud-Aerosol Lidar with Orthogonal Polarization; CALIOP) observations and reanalysis (ECMWF Re-analysis; ERA-Interim) data in five austral winters of 2007–2011. A description of the data used in the present study is made in Sect. 2. Results are shown in Sect. 3; First, statistical analyses of the simultaneous occurrence of PSCs and UCs are made. Second, composite analyses and a detailed case study are made to show that tall structure of blocking highs (BHs) is an important factor for the simultaneous occurrence of PSCs and UCs. Third, after

taking an appropriate definition of blocking highs, similarity of longitudinal distributions of occurrence frequency of BHs and of simultaneous occurrence of PSCs and UCs is examined. Finally, the fractions of each composition of PSCs are shown as a function of longitude relative to anticyclones. The summary and concluding remarks are given in Sect. 4.

## 2 Data description

In the present analysis, the Lidar Level 1B Profile data product (version 3) from Cloud-Aerosol Lidar and Infrared Pathfinder Satellite Observations (CALIPSO) is used to examine PSCs and UCs. This data product includes profiles of total attenuated backscatter and perpendicular attenuated backscatter at 532 nm in the altitude range up to 40.0 km and covers the latitudinal region of 82° S–82° N. An algorithm proposed by Pitts et al. (2009) is used for detecting PSCs. Moreover, following Pitts et al. (2009), only nighttime data are analyzed for 55° S–82° S where most PSCs are observed. As it is not clear whether UCs are actually clouds in the troposphere, the occurrence frequency of clouds is defined as the percentage of cases where any cloud (PSC or UC) was observed. The occurrence frequency of clouds (hereinafter referred to as PSC/UC frequency) is calculated for each day in the regions with longitude intervals of 10° for five latitude bands of (55° S, 60° S), (60° S, 65° S), (65° S, 70° S), (70° S, 75° S) and (75° S, 82° S).

While the algorithm was originally intended to categorize PSCs in 400 K–700 K potential temperature levels, Alexander et al. (2010) suggested that the same PSC detection algorithm can be applied for the region extended down to a 350 K level based on the fact that the PSC distributions in 350–400 K levels are similar to those in the upper layer. To examine PSCs in the lowermost stratosphere and UCs without distinction, the present study further applied the same algorithm to the region down to 300 K using the same algorithm. Thus we analyzed any cloud in the region of potential temperatures from 300 K to 700 K (~8–28 km in polar latitudes) and refer it to as “PSC/UC”.

## Polar stratospheric clouds and upper-tropospheric clouds

M. Kohma and K. Sato

Title Page

Abstract

Introduction

Conclusions

References

Tables

Figures



Back

Close

Full Screen / Esc

Printer-friendly Version

Interactive Discussion



---

## Polar stratospheric clouds and upper-tropospheric clouds

M. Kohma and K. Sato

---

Title Page

Abstract

Introduction

Conclusions

References

Tables

Figures

⏪

⏩

◀

▶

Back

Close

Full Screen / Esc

Printer-friendly Version

Interactive Discussion



To ensure that the algorithm works in the lowermost stratosphere and upper troposphere, a Hovmöller diagram of PSC/UC frequency in 9–11 km was made for June through September (Fig. 1a). For comparison, the plot of PSC/UC frequency made from CALIPSO Level 2 Vertical Feature Mask (VFM) data is also shown (Fig. 1b). The VFM data product categorizes each segment into a feature type: “clear air”, “cloud”, and “stratospheric”. In calculation of PSC/UC frequency, both “cloud”, and “stratospheric” feature types are used in the present study. The distributions observed in these two plots are quite similar, indicating that the algorithm by Pitts et al. can be used to detect clouds in the region down to the 300 K level correctly in terms of the occurrence frequency.

In addition, based on inverse scattering ratios and depolarization ratios, PSCs are categorized into four groups: ice, STS (super-cooled ternary solution), Mix1 (mixture of lower number/volume of NAT particles and STS particles) and Mix2 (mixture of higher number/volume of NAT particles and STS particles) (Pitts et al., 2009). Pitts et al. (2009) categorized PSC compositions in the two dimensional space of the inverse scattering ratio versus the depolarization ratio, assuming the typical conditions at 50 hPa (~22 km) for the HNO<sub>3</sub> and H<sub>2</sub>O mixing ratios. Thus, the PSC composition below 15 km (~400 K) is not examined in the present study.

Daily-mean ERA-Interim data are used for the analysis of atmospheric disturbances. The tropopause is determined based on isentropic potential vorticity (PV). As indicated by Gettelman et al. (2011), this tropopause definition may not be appropriate, because the PV value representing the tropopause changes seasonally. However, according to Kunz et al. (2011), a PV value of  $-2$  PVU (PVU =  $10^{-6} \text{ m}^2 \text{ s}^{-1} \text{ K kg}^{-1}$ ) roughly corresponds to the PV gradient-based tropopause in high-latitudes of the Southern Hemisphere. Thus, the present study used the definition by Kunz et al. for the dynamical tropopause height.

### 3 Results

#### 3.1 The relation between PSCs and UCs

The right panel of Fig. 2 shows zonally-averaged PSC/UC frequencies as a function of altitude for 70° S–75° S from June through September 2008. Note that discontinuity around 20 km is due to the difference in the original vertical resolution of CALIPSO Level 1 data below and above the level and should be ignored. A relatively high frequency is observed in 14–25 km and below 10 km while PSC/UC frequencies are low around 13 km.

To examine how often PSCs and UCs simultaneously occur, correlation coefficients ( $r$ ) between the time series of the PSC/UC flag showing whether PSC/UC are observed or not at two different altitudes are calculated (the left panel of Fig. 2). The correlation coefficients greater than about 0.09 are statistically meaningful at a significance level of 99 %. It is found that the time series for 15–25 km are positively correlated with those for 15–25 km and for 9–11 km with  $r$  greater than 0.1. Correlation coefficients of clouds for 15–25 km and those below 9 km are lower than 0.09. An interesting feature is that the correlation is minimized around 13 km. These features indicate that the PSC/UCs in 15–25 km and those in 9–11 km are separated but related by a remote mechanism. On the other hand, the time series for 9–11 km are positively correlated with those below 20 km and the minimum correlation coefficient are not clear around 13 km. It is noticeable that the minimum of correlation may be related to that of vertical profile of averaged PSC frequency shown in Fig. 2b.

It is likely that the PSC/UCs in 15–25 km and those in 9–11 km respectively correspond to simultaneously occurring PSCs and UCs as indicated by previous studies (e.g. Wang et al., 2008). However, it should be emphasized here that a typical tropopause height in the polar winter is  $\sim 7$ –8 km, which can be lower than the UC altitudes even taking it into consideration that the tropopause level is modified by atmospheric disturbances. Nevertheless, as a matter of convenience, we refer to the

## Polar stratospheric clouds and upper-tropospheric clouds

M. Kohma and K. Sato

Title Page

Abstract

Introduction

Conclusions

References

Tables

Figures

⏪

⏩

◀

▶

Back

Close

Full Screen / Esc

Printer-friendly Version

Interactive Discussion



PSC/UCs in 15–25 km as PSCs and those in 9–11 km as UCs in the following analyses.

Figure 3 shows zonally-averaged PSC/UC frequency as a function of altitude (right panels) and cross-correlation maps (left panels) for 70° S–75° S for respective months of June through September obtained using data for five years of 2007–2011. The correlation coefficients greater than about 0.10 are statistically meaningful at a significance level of 99 %.

The minimum of vertical profiles of PSC/UC frequency is seen in an altitude range of 12–14 km in June and July. The minimum gradually becomes obscured with time. This feature is probably related to the seasonal variation of the altitudes where PSCs are observed. According to Pitts et al. (2007), the altitudes where PSCs are dominant lower from 22 km in June and to 15 km or below in September and October following the lowest temperature descent.

Time series of PSCs in 17–23 km are positively correlated with those of UCs in 9–11 km and of PSCs 17–25 km in June with  $r > 0.2$ . In July, time series for 17–25 km are positively correlated with those in the same height range of 17–25 km with  $r > 0.2$ . Correlation coefficients of PSCs in 16–21 km have a small maximum around an altitude of 11 km. In August, PSCs in 15–23 km are not only correlated with those in the same altitude range but also have a stronger correlation ( $r > 0.2$ ) with those of UCs in 9–11 km than in July. In September when PSC frequencies are maximized around an altitude of 17 km with about 10 %, the correlation coefficients of time series of PSCs around 17 km with those of UCs in 9–11 km and of PSCs in 15–20 km are larger than 0.2. In summary, those of PSCs are positively correlated with those of UCs and have a minimum correlation around 13 km in any month.

Time series of UCs in 9–11 km are positively correlated with those below 20 km in July through September. It is important to note that the correlation coefficients of time series of UCs are even minimized in 13–15 km ( $r < 0.1$ ) in June, while those of UCs are significantly correlated with those of PSCs in 17–23 km and those of UCs in 9–11 km with  $r > 0.2$ .

## Polar stratospheric clouds and upper-tropospheric clouds

M. Kohma and K. Sato

Title Page

Abstract

Introduction

Conclusions

References

Tables

Figures



Back

Close

Full Screen / Esc

Printer-friendly Version

Interactive Discussion



Time series of PSC/UCs in 13–15 km does not have significant correlation with those of PSCs above 17 km and not with those of UCs in 9–11 km. This fact indicates that there is a gap around 13 km between the UCs and PSCs in terms of the frequency and correlation.

These results in this subsection suggest that PSCs in 15–25 km frequently occur simultaneously with UCs in 9–11 km and not with clouds around 13 km. The cloud gap around 13 km is particularly clear in June. This cloud gap is also seen in snap shots shown by previous case studies (e.g. Fig. 3 in Wang et al., 2008).

### 3.2 Tropospheric anticyclones and simultaneously appearing PSCs and UCs

Previous studies indicate that PSCs are sometimes observed in association with anticyclonic PV anomalies near the tropopause (Teitelbaum et al., 2001; Kohma and Sato, 2011). Figure 4 shows a composite of the altitude and relative-longitude section of PSC/UC frequencies for 70° S–75° S for June through August of 2008. Here we take a reference longitude at which the PV anomaly from the zonal mean at 72.5° S on 300 K is positively maximized with a value greater than 1.5 PVU. The PSC/UC frequencies are interpolated linearly into 1.5° in the longitudinal direction. Significantly-high frequencies are seen around the dynamical tropopause denoted by a red curve (~9–10 km) around the reference longitude. High frequencies are also observed in 15–20 km in the similar longitude range. These features suggest that the simultaneous occurrence of PSCs and UCs is associated with anticyclones near the tropopause.

Note that the dynamical tropopause is slightly elevated around the reference longitude of the anticyclonic PV anomaly as is consistent with a theoretical study by Wirth (2000). The UCs are observed around and even slightly above the elevated tropopause (i.e. in the stratosphere). The fact indicates that it is more appropriate to call them “tropopausal” clouds instead of UCs.

Figure 5a shows a typical example of concurrent occurrence of PSCs and UCs over the Antarctic Peninsula along a CALIPSO orbit on 2 August 2008. The PSC/UCs are observed along the orbit of (62° S, 67° W) to (78° S, 93° W) in altitude ranges of 15–

20015

## Polar stratospheric clouds and upper-tropospheric clouds

M. Kohma and K. Sato

Title Page

Abstract

Introduction

Conclusions

References

Tables

Figures



Back

Close

Full Screen / Esc

Printer-friendly Version

Interactive Discussion



25 km and below 12 km. Little PSC/UCs are observed around 14 km, which corresponds to the cloud gap between PSC and UC regions as statistically seen in Fig. 3a. Figure 5b shows a PV map on the 300 K isentropic surface by red contours, geopotential heights at 300 hPa ( $\sim 8$  km) by color and the satellite orbit by a thick broken curve.

5 An anticyclone with a horizontal scale larger than 3000 km is located over the Antarctic Peninsula. The longitude-pressure section of geopotential height anomalies from the zonal mean at  $65^\circ$  S is shown in Fig. 5c. It is clear that an anomaly maximum corresponding to the anticyclone in  $30^\circ$  W– $90^\circ$  W extends vertically up to 30 hPa ( $\sim 22$  km). The temperatures are minimized around the geopotential height maximum and lower than 185 K in 20–60 hPa.

10 Next, it is examined whether the anticyclonic PV anomalies near the tropopause can cause low temperatures in the height range of 15–20 km. First, we considered an ideal situation in which a delta function-like anticyclonic PV anomaly is present at the tropopause in the vertical. This situation is similar to an anticyclonic PV anomaly at the upper boundary in Eady's baroclinic instability theory (e.g. Vallis, 2006). In this case, the e-folding vertical extent of temperature anomaly induced by the PV anomaly is obtained at the Rossby height (Hoskins et al., 1985). The Rossby height  $H_R$  is defined as  $fL/2\pi N$ , where  $f$  is Coriolis parameter,  $N$  is static stability, and  $L$  is horizontal wavelength ( $= 2\pi/k$ ,  $k$  is horizontal wavenumber). In winter high-latitudes, a typical  $H_R$  value is estimated at about 5 km in the lowermost stratosphere, taking  $N = 0.02 \text{ s}^{-1}$  and  $L = 5000$  km as typical values. As the tropopause is climatologically located around a height of 8 km, the temperature anomalies should have significant amplitudes only up to 13 km. Even if we consider the elevation of the tropopause by about 2 km associated with the anticyclone as seen in Fig. 4, the vertical extent cannot reach the height of 15 km. Thus, the anticyclonic PV anomalies confined to the tropopause are hardly attributable to the existence of PSCs in the height range of 15–20 km range.

25 Next, the anticyclonic PV anomaly with a finite depth was considered. An analysis was made of PV distribution in terms of equivalent latitudes  $y_e$  (dynamical latitudes defined based on PV) (Butchart and Remsberg, 1985) using ERA-Interim data on 2

## Polar stratospheric clouds and upper-tropospheric clouds

M. Kohma and K. Sato

Title Page

Abstract

Introduction

Conclusions

References

Tables

Figures

⏪

⏩

◀

▶

Back

Close

Full Screen / Esc

Printer-friendly Version

Interactive Discussion



August 2008. Figure 5d shows a geographical latitude-pressure section of the equivalent latitudes at 60° W. An important feature is that the air with equivalent latitudes lower than 60° S intrudes into a geographical latitude of 67° S in the troposphere having a vertical extent up to 100 hPa (about 15 km) (see contour lines of  $y_e = 60^\circ \text{ S}$ ).

5 Taking a height of 15 km as the top edge of the tropospheric disturbances, the vertical penetration is estimated at 20 km using Rossby height ( $\sim 5$  km) for typical values and real values for this case of  $N = 0.02 \text{ s}^{-1}$  and  $L = 5000$  km. Thus, the anticyclonic disturbance with a large horizontal scale and tall structure as observed in Figs. 4 and 5b–d can cause low temperatures in the entire altitude range where PSCs as well as  
10 UCs are observed. These characteristic large horizontal and vertical spatial structures suggest that the anticyclonic disturbances are likely due to BHs in the troposphere (e.g. Schwierz et al., 2004).

Wang et al. (2008) pointed out that tropospheric cyclones are a possible candidate causing the concurrent occurrence of PSCs and UCs. They speculated that the vertical material transport associated with tropospheric cyclones is responsible for the  
15 occurrence of PSCs and that the intense cyclones are typically accompanied by high clouds above 7 km. We examined meteorological situation for the case of PSCs and UCs shown in Wang et al. (2008) (their Fig. 3), and confirmed that a blocking high was present instead of a cyclone.

20 It is worth noting that the cloud gap around 14 km, which are observed in Fig. 5a, cannot be explained only by this mechanism. We need to consider an additional factor. A plausible candidate is the supply of  $\text{H}_2\text{O}$  rich air from the troposphere to the cold stratosphere mixing process. Based on trajectory analyses, Pfister et al. (2003) showed that the troposphere-stratosphere exchange extends to about 13 km in the Arctic winter and that mixing ratios of  $\text{H}_2\text{O}$  can be significantly higher than a typical value of 5 ppmv  
25 in the stratosphere. Such humid air supply may be a necessary condition for simultaneous occurrence of PSCs and UCs in addition to the low temperature associated with the anticyclones having deep structure. The reason that little clouds are formed around 13 km is likely that humid air from the troposphere reaches up to an altitude of 13 km.

## Polar stratospheric clouds and upper-tropospheric clouds

M. Kohma and K. Sato

Title Page

Abstract

Introduction

Conclusions

References

Tables

Figures



Back

Close

Full Screen / Esc

Printer-friendly Version

Interactive Discussion



### 3.3 Longitudinal dependencies of blocking highs and simultaneous occurrence of PSCs and UCs

In this section, the occurrence frequency of BHs is estimated using daily-mean ERA-interim data based on a method similar to the criteria suggested by Schwierz et al. (2004). First, analyzed area is limited to a latitude range of 55° S–85° S, where PSCs are mainly observed. Second, equivalent latitudes vertically-averaged for isentropic levels of 300–320 K (hereafter referred to as AELs) are obtained for each day, because the blocking highs have tall structure (Schwierz et al., 2004). Third, the regions surrounded by 55° S AEL contours and/or a geographic latitude circle of 55° S are obtained as candidate BHs (CBHs). Last, the BHs are selected from CBHs by posing the following two criteria: the horizontal area is greater than  $3 \times 10^6 \text{ km}^2$ , and the southernmost geographical latitude of CBH is higher than 65° S. The threshold of the former criterion was chosen to examine the spatial scales corresponding to  $H_R \sim 4 \text{ km}$  at 65° S. The latter criterion ensures that the areal extent of BH covers high latitudes where the PSCs are frequently observed. The obtained BH area amounts to about 15% of the latitudinal region of 55° S–82° S in June through September on average. This fact means that the BHs having a potential to cause PSC/UC are not rare disturbances.

The height region of 15–25 km is separated into the two because spatial of the Level 1 data of CALIPSO above and below 20 km are different. Table 1a shows numbers of the simultaneous occurrence of PSCs and UCs accompanying BHs and in the absence of the BHs in 60° S–75° S in the 5 austral winters. Observations in the latitude range of 75° S–82° S are not used in the following analyses, because PSCs are almost always observed in July through August due to sufficiently low temperatures regardless of the BH presence. The simultaneous occurrence of PSCs and UCs is defined as the cases when both PSC/UC frequencies in 9–11 km and 15–20 km are greater than 10%. From Table 1a, it is found that about a half of the concurrent occurrence of PSCs and UCs is

## Polar stratospheric clouds and upper-tropospheric clouds

M. Kohma and K. Sato

Title Page

Abstract

Introduction

Conclusions

References

Tables

Figures



Back

Close

Full Screen / Esc

Printer-friendly Version

Interactive Discussion



associated with BHs. This value is about 3 times higher than that for the case without BHs.

The numbers of simultaneous occurrence of PSCs in 20–25 km and UCs in 9–11 km are shown in Table 1b. The numbers of each case are quite similar to those in Table 1a although the numbers of simultaneous occurrence in Table 1b are slightly smaller than those in Table 1a. Thus, our analyses in this section focus on simultaneous occurrence of PSCs in 15–20 km and UCs in 9–11 km.

The frequency of the simultaneous occurrence of PSCs and UCs (black solid curves) and that of BHs (red broken curves) are shown as a function of longitude in Fig. 6 for the 5 austral winters. The frequency of BHs are higher than that of simultaneous occurrence of PSCs and UCs in 120° E to 90° W in 2007 while they are quite similar in the other longitude region. The similar features are seen in the other years. The correlation coefficients are lower than 0.2 in 2007, 2008, 2009 and 2011 whereas it is 0.56 in 2010.

Next, the frequency of BHs is calculated for the region only inside the polar vortex on a 500 K isentropic surface in the middle stratosphere (red solid curves). Here, the edge of the polar vortex is determined based on PV following Nash et al. (1996). The longitudinal variation of BH frequency inside the polar vortex more resembles that of the frequency of simultaneous occurrence of PSCs and UCs, particularly for 120° E–90° W. The correlation coefficients increase to 0.56, 0.72, 0.36, 0.79 and 0.29 in 2007, 2008, 2009, 2010 and 2011, respectively. These results indicate that the tropospheric BHs provide preferable conditions for the simultaneous occurrence of PSCs and UCs inside the stratospheric polar vortex.

Previous studies (e.g. Kohma and Sato, 2011) showed that PSCs are more frequently observed over the Antarctic Peninsula than in the other regions. Several studies indicated that cold phase of temperature fluctuations associated with mountain waves originated from the Antarctic Peninsula increases the formation of ice particles, on which the heterogeneous nucleation of NAT particles can occur (Carslaw et al., 1998; Höphner et al., 2006; Eckermann et al., 2009). Because NAT particles have higher

## Polar stratospheric clouds and upper-tropospheric clouds

M. Kohma and K. Sato

Title Page

Abstract

Introduction

Conclusions

References

Tables

Figures



Back

Close

Full Screen / Esc

Printer-friendly Version

Interactive Discussion



equilibrium temperature than the ice frost point, occurrence frequency of PSCs over Antarctic Peninsula can rise. It is an important and interesting feature in Fig. 6 that the frequency of PSC is large in the longitude region ( $80^{\circ}\text{W}$ – $120^{\circ}\text{W}$ ) even windward of the Antarctic Peninsula ( $60^{\circ}\text{W}$ – $70^{\circ}\text{W}$ ). It is not likely that the orographic gravity waves cause low temperatures in such a region. The PSC frequency associated with BHs in latitude range of  $70^{\circ}\text{S}$ – $75^{\circ}\text{S}$  is about 32 % which is significantly higher than the mean PSC frequency (17 %). Therefore, BHs are a strong candidate to cause high PSC frequency to windward of the Antarctic Peninsula (Fig. 6).

### 3.4 Effects of blocking highs on PSC composition

Adhikari et al. (2009) showed that ice PSCs are frequently observed in association with tropospheric cloud systems, especially in late PSC season. Figure 7a shows PSC/UC frequencies as a function of altitude and relative-longitude to the anticyclones in  $70^{\circ}\text{S}$ – $75^{\circ}\text{S}$  in August of 5 austral winters. Significant results were not obtained in September and October due to insufficient number of cases of PSC/UC above an altitude of 15 km. Figures 7b–e show longitude-altitude sections of fraction (%) of PSCs categorized into PSC composition (i.e. STS, Mix1, Mix2 and Ice). It is clear that Mix2 clouds are most dominant, which is consistent with climatological PSC composition in August shown by Pitts et al. (2009).

It is interesting to see the relative longitudes where the fraction of each PSC composition is largest. Note that dominant mean flows are eastward in the polar stratospheric winter. The proportions of Mix1 and Mix2 PSCs are higher to the east of reference longitude, namely, to leeward of the anticyclonic PV. The proportion of Ice PSCs is maximized around the reference longitude (i.e. zero relative-longitude). The proportion of STS is higher to the windward of anticyclonic PV than that to leeward.

Previous studies showed that a significant NAT production is preceded by local but strong cooling associated with gravity waves (ice-seeding process) (Fueglistaler et al., 2002; Höphner et al., 2006; Eckermann et al., 2009; Lambert et al., 2012), i.e. NAT PSCs are nucleated on the ice particles which are produced by the low temperatures

## Polar stratospheric clouds and upper-tropospheric clouds

M. Kohma and K. Sato

Title Page

Abstract

Introduction

Conclusions

References

Tables

Figures



Back

Close

Full Screen / Esc

Printer-friendly Version

Interactive Discussion



in association with the gravity waves. The dependence of PSC composition on relative location between the anticyclone center and PSCs as observed in Fig. 7 may be understood in the same manner of the ice seeding-process by gravity waves but by anticyclones in the present case. Note that this inference is consistent with the study by Larsen et al. (2004) showing that solid particles are strongly affected by the synoptic scale temperature histories rather than local temperatures in Arctic early winter.

#### 4 Summary and concluding remarks

In this study, using satellite lidar data and reanalysis data in five austral winters of 2007–2011, the simultaneous occurrence of PSCs and UCs in the Southern Hemisphere has been examined. In particular, the role of blocking highs was emphasized.

A correlation analysis has shown that PSCs and UCs are dominant in the altitude ranges of 15–24 km and 9–11 km, respectively. PSCs in an altitude range of 18–23 km are positively correlated with UCs in an altitude range of 9–11 km. The cloud existence below 9 km was weakly correlated with those of the PSC and UC. It was also shown that the UCs are located around and slightly above the tropopause (~7–8 km).

The simultaneous occurrence frequencies of the PSCs and UCs were significantly high when BHs appeared in the troposphere. The BH has deep PV anomaly structure causing the negative temperature anomalies vertically extended up to 20 km where PSCs are observed. The frequencies of BHs and of the simultaneous occurrence of PSCs and UCs exhibit similar longitudinal variations, which is much clearer when the analysis of BHs was limited to the region inside the polar vortex on the 500 K isentropic surface. Furthermore, the higher occurrence frequency of PSCs to windward of the Antarctic Peninsula than the other regions can be explained by the distribution of the BH frequency.

It has also been shown that dominant PSC composition depends on the longitude relative to the center of BHs. Ice PSCs are relatively rich above the BHs, while the proportions of NAT-rich and STS-rich PSCs increase to leeward and windward of BHs,

## Polar stratospheric clouds and upper-tropospheric clouds

M. Kohma and K. Sato

Title Page

Abstract

Introduction

Conclusions

References

Tables

Figures



Back

Close

Full Screen / Esc

Printer-friendly Version

Interactive Discussion



respectively. Höpner et al. (2006) discussed the ice-seeding process by extreme low temperature fluctuations associated with gravity waves. The present result suggests that BHs also lead to a similar ice-seeding effect.

A cloud gap exists around 12–15 km, which may also be related to the enhancement of mixing ratios of H<sub>2</sub>O in the lowermost stratosphere due to cross tropopause mixing. This issue should be examined in future studies.

*Acknowledgements.* The CALIPSO data product is provided by NASA Langley Atmospheric Science Data Center for providing the CALIPSO data product. ERA-Interim data are provided by the European Center for Medium Range Weather Forecast (ECMWF). The figures were drawn by the software tools developed under the GFD Dennou Club Davis project. We thank Y. Tomikawa and S. Alexander for their help of treatment of dataset. This study was supported by Grant-in-Aid Scientific Research (B) 22340134 and by Grant-in-Aid for Research Fellow (23–9377) of the JSPS. This manuscript was proofread by a proofreading/editing assistant from the Global COE program, From the Earth to “Earths”.

## References

- Adhikari, L., Wang, Z., and Liu, D.: Microphysical properties of Antarctic polar stratospheric clouds and their dependence on tropospheric cloud systems, *J. Geophys. Res.*, 115, D00H18, doi:10.1029/2009JD012125, 2010.
- Alexander, S. P., Klekociuk, A. R., Pitts, M. C., McDonald, A. J., and Arevalo-Torres, A.: The effect of orographic gravity waves on Antarctic polar stratospheric cloud occurrence and composition, *J. Geophys. Res.*, 116, doi:10.1029/2010jd015184, 2011.
- Butchart, N. and Remsberg, E. E.: The area of the stratospheric polar vortex as a diagnostic for tracer transport on an isentropic surface, *J. Atmos. Sci.*, 43, 1319–1339, 1986.
- Eckermann, S. D., Hoffmann, L., Höpner, M., Wu, D. L., and Alexander, M. J.: Antarctic NAT PSC belt of June 2003: observational validation of the mountain wave seeding hypothesis, *Geophys. Res. Lett.*, 36, L02807, doi:10.1029/2008GL036629, 2009.
- Fromm, M., Alfred, J., and Pitts, M.: A unified, long-term, high-latitude stratospheric aerosol and cloud database using SAM II, SAGE II, and POAM II/III data: algorithm description, database definition, and climatology, *J. Geophys. Res.*, 108, 4366, doi:10.1029/2002JD002772, 2003.

## Polar stratospheric clouds and upper-tropospheric clouds

M. Kohma and K. Sato

Title Page

Abstract

Introduction

Conclusions

References

Tables

Figures

⏪

⏩

◀

▶

Back

Close

Full Screen / Esc

Printer-friendly Version

Interactive Discussion



---

**Polar stratospheric clouds and upper-tropospheric clouds**M. Kohma and K. Sato

---

[Title Page](#)[Abstract](#)[Introduction](#)[Conclusions](#)[References](#)[Tables](#)[Figures](#)[⏪](#)[⏩](#)[◀](#)[▶](#)[Back](#)[Close](#)[Full Screen / Esc](#)[Printer-friendly Version](#)[Interactive Discussion](#)

Fueglistaler, S., Luo, B. P., Voigt, C., Carslaw, K. S., and Peter, T.: NAT-rock formation by mother clouds: a microphysical model study, *Atmos. Chem. Phys.*, 2, 93–98, doi:10.5194/acp-2-93-2002, 2002.

5 Gettelman, A., Hoor, P., Pan, L. L., Randel, W. J., Hegglin, M. I., and Birner, T.: The extratropical upper troposphere and lower stratosphere, *Rev. Geophys.*, 49, RG3003, doi:10.1029/2011rg000355, 2011.

Holton, J. R.: *An Introduction to Dynamic Meteorology*, 4th ed., Academic Press, Burlington, USA, , 535 pp., 2004.

10 Höpfner, M., Larsen, N., Spang, R., Luo, B. P., Ma, J., Svendsen, S. H., Eckermann, S. D., Knudsen, B., Massoli, P., Cairo, F., Stiller, G., v. Clarmann, T., and Fischer, H.: MIPAS detects Antarctic stratospheric belt of NAT PSCs caused by mountain waves, *Atmos. Chem. Phys.*, 6, 1221–1230, doi:10.5194/acp-6-1221-2006, 2006.

Jensen, E. J., Toon, O. B., Tabazadeh, A., and Drdla, K.: Impact of polar stratospheric cloud particle composition, number density, and lifetime on denitrification, *J. Geophys. Res.*, 107, 8284, doi:10.1029/2001JD000440, 2002.

15 Kohma, M. and Sato, K.: The effects of atmospheric waves on the amounts of polar stratospheric clouds, *Atmos. Chem. Phys.*, 11, 11535–11552, doi:10.5194/acp-11-11535-2011, 2011.

Kunz, A., Konopka, P., Müller, R., and Pan, L. L.: Dynamical tropopause based on isentropic potential vorticity gradients, *J. Geophys. Res.*, 116, D01110, doi:10.1029/2010jd014343, 2011.

20 Lambert, A., Santee, M. L., Wu, D. L., and Chae, J. H.: A-train CALIOP and MLS observations of early winter Antarctic polar stratospheric clouds and nitric acid in 2008, *Atmos. Chem. Phys.*, 12, 2899–2931, doi:10.5194/acp-12-2899-2012, 2012.

Larsen, N., Knudsen, B. M., Svendsen, S. H., Deshler, T., Rosen, J. M., Kivi, R., Weisser, C., Schreiner, J., Mauerberger, K., Cairo, F., Ovarlez, J., Oelhaf, H., and Spang, R.: Formation of solid particles in synoptic-scale Arctic PSCs in early winter 2002/2003, *Atmos. Chem. Phys.*, 4, 2001–2013, doi:10.5194/acp-4-2001-2004, 2004.

25 Lowe, D. and MacKenzie, A. R.: Polar stratospheric cloud microphysics and chemistry, *J. Atmos. Sol.-Terr. Phys.*, 70, 13–40, doi:10.1016/j.jastp.2007.09.011, 2008.

30 Nash, E. R., Newman, P. A., Rosenfield, J. E., and Schoeberl, M. R.: An objective determination of the polar vortex using Ertel's potential vorticity, *J. Geophys. Res.*, 101, 9471–9478, doi:10.1029/96JD00066, 1996.

## Polar stratospheric clouds and upper-tropospheric clouds

M. Kohma and K. Sato

Title Page

Abstract

Introduction

Conclusions

References

Tables

Figures

⏪

⏩

◀

▶

Back

Close

Full Screen / Esc

Printer-friendly Version

Interactive Discussion



- Palm, S. P., Fromm, M., and Spinhirne, J.: Observations of antarctic polar stratospheric clouds by the Geoscience Laser Altimeter System (GLAS), *Geophys. Res. Lett.*, 32, L22S04, doi:10.1029/2005gl023524, 2005.
- 5 Pfister, L., Selkirk, H. B., Jensen, E. J., Podolske, J., Sachse, G., Avery, M., Schoeberl, M. R., Mahoney, M. J., and Richard, E.: Processes controlling water vapor in the winter Arctic tropopause region, *J. Geophys. Res.*, 108, 8314, doi:10.1029/2001jd001067, 2002.
- Pitts, M. C., Thomason, L. W., Poole, L. R., and Winker, D. M.: Characterization of Polar Stratospheric Clouds with spaceborne lidar: CALIPSO and the 2006 Antarctic season, *Atmos. Chem. Phys.*, 7, 5207–5228, doi:10.5194/acp-7-5207-2007, 2007.
- 10 Pitts, M. C., Poole, L. R., and Thomason, L. W.: CALIPSO polar stratospheric cloud observations: second-generation detection algorithm and composition discrimination, *Atmos. Chem. Phys.*, 9, 7577–7589, doi:10.5194/acp-9-7577-2009, 2009.
- Schwierz, C., Croci-Maspoli, M., and Davies, H. C.: Perspicacious indicators of atmospheric blocking, *Geophys. Res. Lett.*, 31, L06125, doi:10.1029/2003gl019341, 2004.
- 15 Solomon, S.: Stratospheric ozone depletion: a review of concepts and history, *Rev. Geophys.*, 37, 275–316, 1999.
- Teitelbaum, H., Moustouli, M., and Fromm, M.: Exploring polar stratospheric cloud and ozone minihole formation: the primary importance of synoptic-scale flow perturbations, *J. Geophys. Res.*, 106, 28173–28188, doi:10.1029/2000JD000065, 2001.
- 20 Vallis, G. K.: *Atmospheric and Oceanic Fluid Dynamics: Fundamentals and Large-Scale Circulation*, Cambridge University Press, Cambridge, UK, 2006.
- Wang, Z., Stephens, G., Deshler, T., Trepte, C., Parish, T., Vane, D., Winker, D., Liu, D., and Adhikari, L.: Association of Antarctic polar stratospheric cloud formation on tropospheric cloud systems, *Geophys. Res. Lett.*, 35, L13806, doi:10.1029/2008gl034209, 2008.
- 25 Wirth, V.: Thermal versus dynamical tropopause in upper-tropospheric balanced flow anomalies, *Q. J. Roy. Meteorol. Soc.*, 126, 299–317, doi:10.1002/qj.49712656215, 2000.

## Polar stratospheric clouds and upper-tropospheric clouds

M. Kohma and K. Sato

Title Page

Abstract

Introduction

Conclusions

References

Tables

Figures

⏪

⏩

◀

▶

Back

Close

Full Screen / Esc

Printer-friendly Version

Interactive Discussion



**Table 1.** (a) Numbers of simultaneous occurrence of PSCs in 15–20 km and UCs in 9–11 km in the presence or absence of blocking highs. (b) Same as (a) but for PSCs in 20–25 km and UCs in 9–11 km.

(a)	2007		2008		2009		2010		2011	
Simultaneous PSC & UC	Yes	No								
BH	714	1912	606	1432	705	1962	500	1453	620	1708
No BH	791	6680	728	5941	964	6358	707	7128	597	5132
(b)	2007		2008		2009		2010		2011	
Simultaneous PSC & UC	Yes	No								
BH	672	1954	556	1482	696	1971	330	1623	603	1725
No BH	610	6861	690	5979	828	6494	469	7366	711	5018



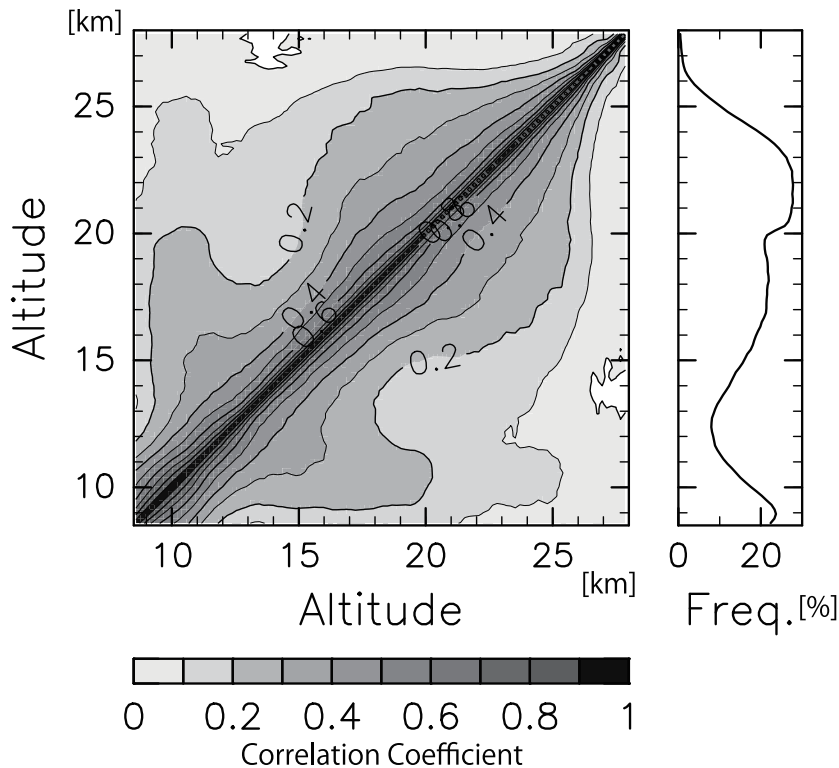


**Fig. 2.** Correlation coefficients between the time series of PSC/UC existence as a function of two altitudes from June through September 2008 (left). The correlation coefficients greater than about 0.09 are statistically meaningful at a significance level of 99%. The right panel shows PSC/UC frequency as a function of altitude (%).

## Polar stratospheric clouds and upper-tropospheric clouds

M. Kohma and K. Sato

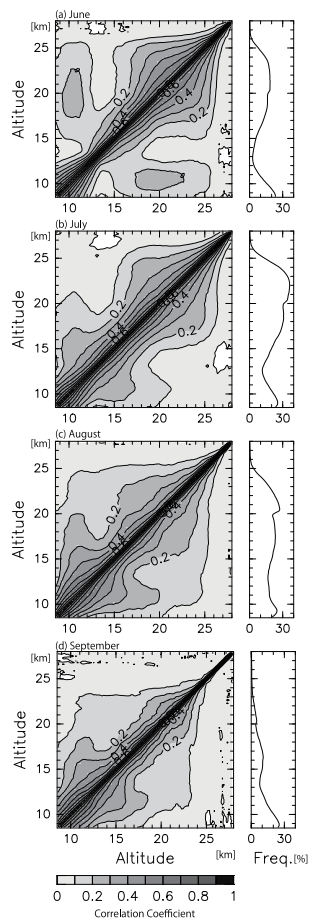


**Fig. 3.** Same as Fig. 2 but for (a) June, (b) July, (c) August, (d) September in 2007–2011. The correlation coefficients greater than about 0.10 are statistically meaningful at a significance level of 99 %.

## Polar stratospheric clouds and upper-tropospheric clouds

M. Kohma and K. Sato

Title Page

Abstract

Introduction

Conclusions

References

Tables

Figures

◀

▶

◀

▶

Back

Close

Full Screen / Esc

Printer-friendly Version

Interactive Discussion

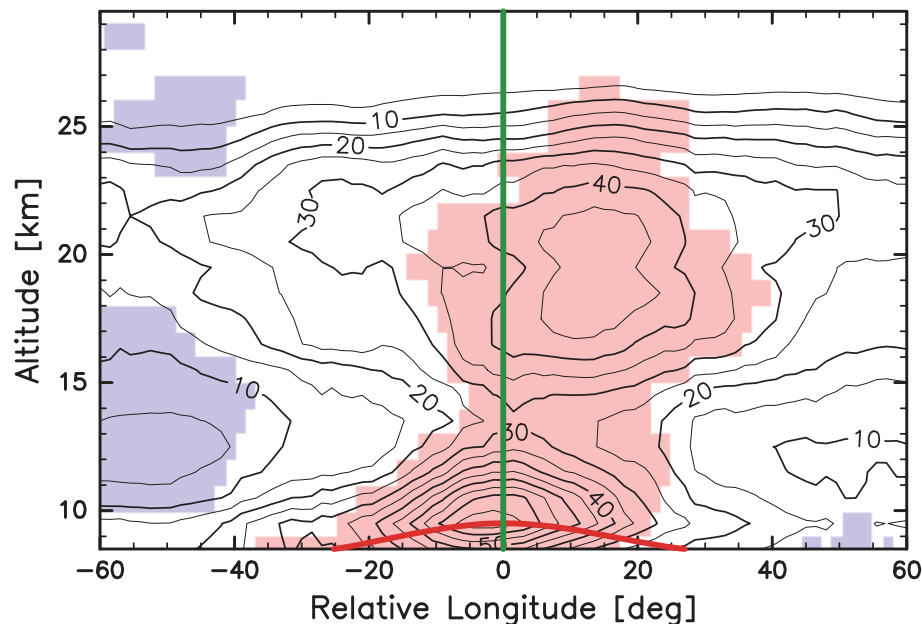


**Fig. 4.** A composite relative-longitude and altitude section of PSC/UC frequency from June through August 2008 with a reference longitude (the green curve) where PV anomalies from the zonal mean are positive and maximized in the zonal direction at  $72.5^{\circ}$  S on a 300 K-isentropic surface, and their values are larger than 1.5 PVU. The number of cases used for the composite is 107. Contour intervals are 5%. Red-shaded (blue-shaded) are the regions with PSC/UC frequency higher (lower) than averaged values and significance levels greater than 95%. The red thick curve indicates the composite of the dynamical tropopause ( $PV = -2$  PVU).

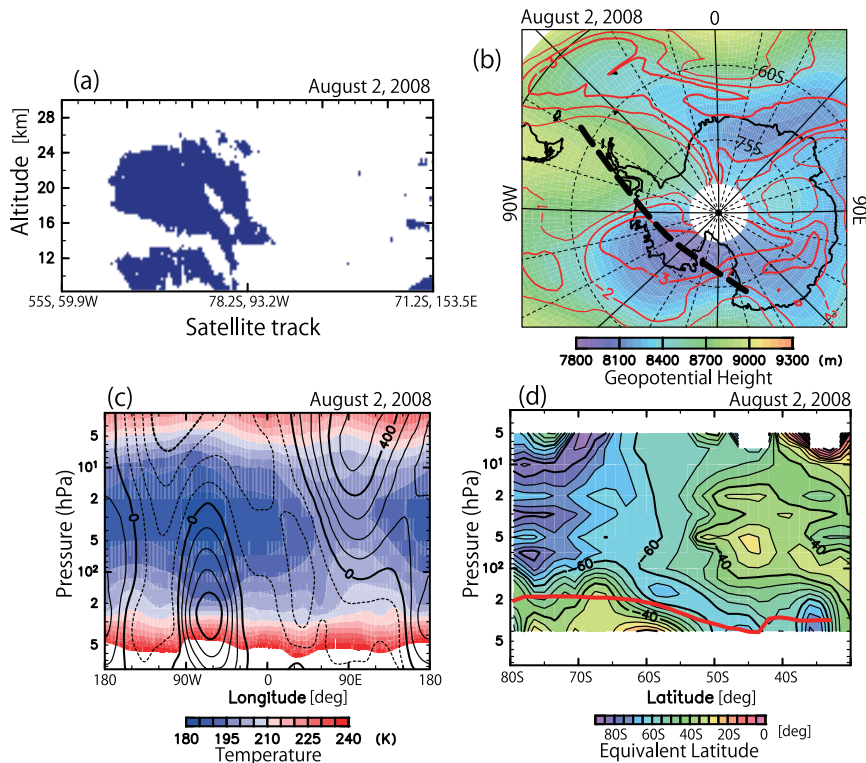


**Fig. 5.** (a) A horizontal and height section of the location of PSC/UC flag (blue color) from CALIPSO on 2 August 2008. (b) A polar stereo projection map of geopotential heights (color, unit is m) at 300 hPa and PV (red contour, unit is PVU) on a 300 K isentropic surface. Contour intervals are 1 PVU. The broken thick curve indicates the satellite track in (a). (c) A longitude and pressure section of geopotential height anomalies from the zonal mean (m) in contours and temperature anomalies from the zonal mean (K) in color at 65° S. Contour intervals are 100 m. Broken contours indicate negative values. (d) A geographical latitude and pressure section of equivalent latitudes at 60° W. The red curve shows dynamical tropopause (PV = -2 PVU).

## Polar stratospheric clouds and upper-tropospheric clouds

M. Kohma and K. Sato

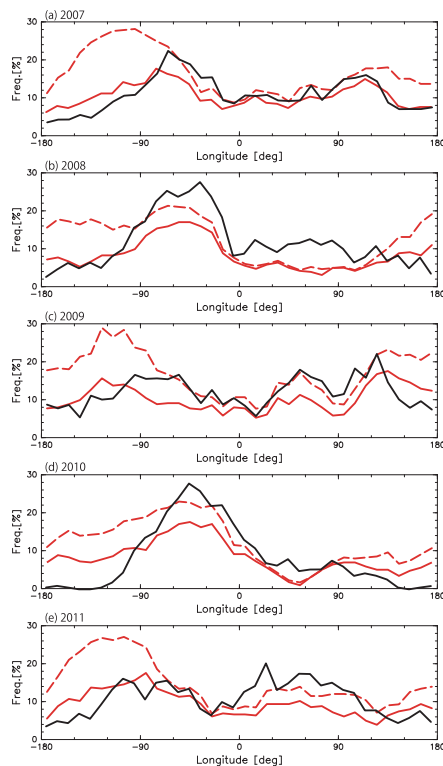


**Fig. 6.** Black curves show frequencies of simultaneous observations of PSCs in the altitude range of 15–20 km and UCs between 9–11 km as a function of longitude in June through September **(a)** 2007, **(b)** 2008, **(c)** 2009, **(d)** 2010 and **(e)** 2011. Red broken curves indicate frequencies of blocking highs south of 60° S. Red solid curves show frequencies of blocking highs calculated for the region only inside the polar vortex on 500 K isentropic surface.

[Title Page](#)[Abstract](#)[Introduction](#)[Conclusions](#)[References](#)[Tables](#)[Figures](#)[◀](#)[▶](#)[◀](#)[▶](#)[Back](#)[Close](#)[Full Screen / Esc](#)[Printer-friendly Version](#)[Interactive Discussion](#)

## Polar stratospheric clouds and upper-tropospheric clouds

M. Kohma and K. Sato

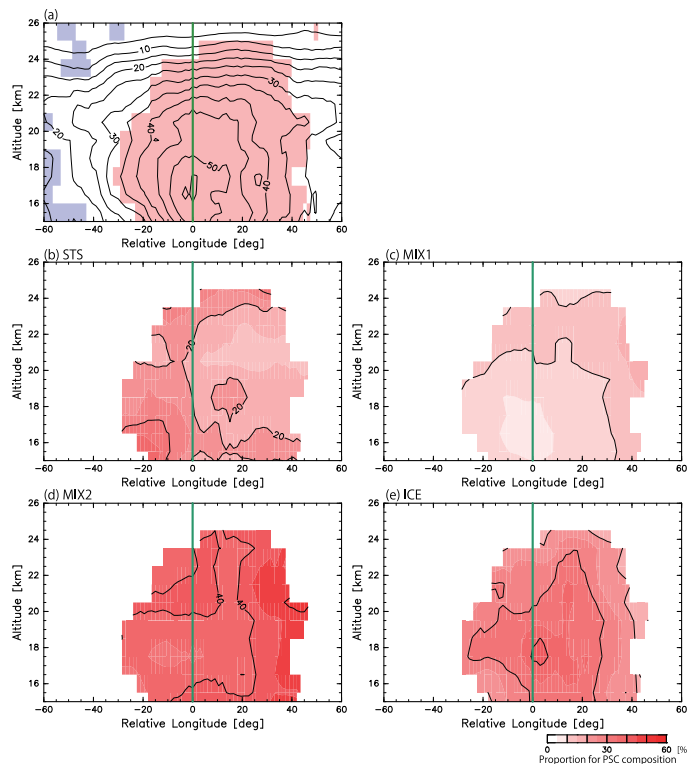


**Fig. 7.** (a) Same as Fig. 4 but for August of 2007–2011. The number of cases used for the composite is 107. (b)–(d) Same as (a) but for proportion for each PSC composition: (b) STS, (c) Mix1, (d) Mix2 and (e) Ice. Coloring corresponds to significantly-high PSC/UC frequency region in (a).

Title Page

Abstract

Introduction

Conclusions

References

Tables

Figures

◀

▶

◀

▶

Back

Close

Full Screen / Esc

Printer-friendly Version

Interactive Discussion